Mice lacking uPA, tPA or Plasminogen genes are resistant to experimental choroidal neovascularization

Lambert V[1*], Munaut C[1*], Bajou K[1*], Peyrollier K[1*], Alvarez-Gonzalez M-L[1*], Carmeliet P[2], Foidart J-M[1*], Noël A[1*] and Rakic J-M[3]

[1]Laboratory of Tumor and Development Biology, ULg, [2]Center for Transgene and Gene Therapy, KUL, [3]Department of Ophthalmology, ULg, BELGIUM.
[*]Center of Experimental Cancer Research (CRCE), ULg, BELGIUM.

A- ABSTRACT

Pathological angiogenesis is the underlying cause of the exsudative form of age-related macular degeneration (AMD). Unlike retinal neovascularization, choroidal neovascularization (CNV) is not primarily induced by hypoxia and the molecular signals involved in its initiation and progression are only partly defined. Angiogenesis is an invasive process that requires proteolysis of the extracellular matrix, proliferation and migration of endothelial cells with simultaneous synthesis of new matrix components. Such migratory and tissue remodeling events are regulated by different proteolytic systems including matrix metalloproteinases (MMPs) and serine proteinases of the plasminogen/plasminogen activator (Plg/PA) system.
Urokinase-type (uPA), which binds to a cellular receptor (uPAR), and tissue-type (tPA) plasminogen activators, are serine proteases both able to activate the zymogen plasminogen (Plg) into plasmin. Plasmin is a broadly acting enzyme, which degrades fibrin, extracellular matrix proteins, and activates pro-MMPs and growth factors. Plasminogen activator inhibitor type 1 (PAI-1) is the main physiological inhibitor of PA.
Vascular endothelial growth factor (VEGF) induces uPA and tPA in endothelial cells derived from the microvasculature and when endothelial cells migrate, they significantly upregulate uPA, tPA, uPAR and PAI-1 at the leading edge of migration. The importance of PAI-1 in the "proteolytic balance" has been demonstrated *in vitro* and in tumoral angiogenesis. The specific roles of the Plg/PA system remain however more controversial.
Since neovascularization has been reported to occur upon fibrin degradation in exsudative AMD, we investigated here the expression and activity of members of the fibrinolytic system in human and laser-induced murine choroidal neovascularization. The influence of endogenous uPA, uPAR, tPA and Plg on CNV formation was further evaluated in single gene deficient mice compared to wild-type (WT) controls.

B- MATERIALS AND METHODS

RT-PCR analysis of neovascular membranes
Eight consecutive submacular CNV specimens were completely removed during surgery for 360° macular translocation performed on patients with exsudative AMD (3 male, 5 female, mean age 77 yrs, range 72-83) either not amenable to conventional laser/ photodynamic therapy (presence of occult newvessels or submacular bleeding) or for one patient, due to a large recurrence occurring a few months after a successful medical treatment. The neovascular membranes were snap frozen in liquid nitrogen and stored at –80°C. The methods conform to the Declaration of Helsinki for research involving human subjects.
Choroidal neovascularization was induced in mice by multiple argon laser burns as previously described. Animals were sacrified at day 3, 5, 10, 14, 20, 40 and the eyes were enucleated. The posterior segments (neural retina and RPE-choroid complex) were cut out and immediately frozen in liquid nitrogen.
The frozen tissues were first pulverized using a Dismembrator (B. Braun Biotech international, Gmbh Melsungen, Germany) and total RNA were extracted with the RNeasy extraction kit (Quiagen, Paris, France) according to the manufacturer's protocol. 28S rRNA were amplified with an aliquot of 10 ng of total RNA using the GeneAmp Thermostable rTth reverse transcriptase RNA PCR kit (Applied Biosystems, Foster City, California) and two pairs of primers (Eurogentec, Liège, Belgium, oligonucleotides sequences are shown in Table1). Reverse transcription was performed at 70°C for 15 min followed by 2 min incubation at 95°C for denaturation of RNA-DNA heteroduplexes. Amplification started by 15 sec at 94°C, 20 sec at 60°C and 10 sec at 72°C. RT-PCR products were resolved on 2% agarose gels and analysed using a Fluor-S Multimager (BioRad) after staining with ethidium bromide (FMC BioProducts).

Murine model of laser-induced choroidal neovascularization
Choroidal neovascularization was induced in mice by four burns (at the 6, 9, 12, and 3 o'clock positions around the optic disc) using a green argon laser (532 nm; 50 µm diameter spot size; 0.05 sec duration; 400 mW). The eyes were enucleated at day 14, embedded in Tissue Tek (Miles Laboratories, Naperville, Illinois) and frozen in liquid nitrogen for cryostat sectioning. Briefly, frozen serial sections were cut throughout the entire extent of each burn, and the thickest region (minimum of 4/lesion) used for the quantification. Using a computer-assisted image analysis system (Olympus Micro Image version 3.0 for Windows 95/NT, Olympus Optical CO. Europe GmBH), neovascularization was estimated by the ratio (B/C) of the thickness from the bottom of the pigmented choroidal layer to the top of the neovascular membrane (B) to the thickness of the intact-pigmented choroid adjacent to the lesion (C).

Genetically modified mice
Brother-sister mating generated all knockout mice in a C57B16/129 background and their corresponding WT littermates. Homozygous deficient mice for uPA ($uPA^{-/-}$), tPA ($tPA^{-/-}$), uPAR ($uPAR^{-/-}$), Plg ($Plg^{-/-}$) and their corresponding WT with a mixed genetic background of 75% C57B16 and 25% 129 SV/SL strain were generated as described previously[21-23]. Mice of either sex between 8 and 12 week old were used. There were five or more mice in each group. The animals were maintained with a 12-h light/12-h dark cycle and had free access to food and water. All the animal experiments were performed in compliance with the Association for Research in Vision and Ophthalmology (ARVO) statement for the Use of Animals in Ophthalmic and Vision Research.

Immunohistochemistry
Cryostat sections (5µm thick) were fixed in paraformaldehyde 1% in 0.07M phosphate buffered saline (PBS) pH 7.0 for 5 min or in acetone for 10 min at room temperature and then incubated with the primary antibody. Antibodies raised against type IV collagen (guinea pig polyclonal, produced in our laboratory; diluted 1/100), mouse PECAM (rat monoclonal, PharMingen, San Diego, California; diluted 1/20), murine uPA (rabbit polyclonal, a generous gift of P. Carmeliet, Katholieke Univerziteit Leuven; diluted 1/500), murine tPA (rabbit polyclonal, a generous gift of P. Carmeliet; diluted 1/500), murine uPAR (rabbit polyclonal, a generous gift of S. Rosenberg, Chiron Corporation, Emeryville, USA; diluted 1/500) and murine fibrinogen/fibrin (goat polyclonal, Nordic Immunological, Tilburg, The Netherlands; diluted1/400) were incubated for 1 hr at room temperature. The sections were washed in PBS (3X 10 min) and appropriate secondary antibody conjugated to peroxydase (HRP), tetramethyl-rhodamine isothiocyanate (TRITC) or fluorescein-isothiocyanate (FITC) were added: rabbit anti-goat IgG (Dako, Glostrup, Denmark, diluted 1/100), rabbit anti-rat IgG (Sigma-Aldrich; diluted 1/40), swine anti-rabbit IgG (Dako; diluted 1/200), monoclonal anti-guinea pig IgG (Sigma-Aldrich, Belgium; diluted 1/200) were applied for 30 min. For staining of fibrinogen/fibrin, a drop of AEC+ (Dako, 3-amino-9-ethylcarbazole) was added and sections were counterstained for 1 minute in haematoxylin. For immunofluorescence staining, after 3 washes in PBS for 10 min each and a final rinse in 10 mM Tris-HCl buffer, pH 8.8, labelling was analysed under an inverted microscope equipped with epifluorescence optics. Specificity of staining was assessed either by substitution of nonimmune serum for primary antibody or by testing in the deficient animal.

***In situ* casein zymography**
Cryostat sections were coated with a mixture containing 2% skim milk, 0.9% agar and 600µl of Plg (Sigma-Aldrich). An 8% milk stock solution was prepared in PBS, heated at 95°C for 30 min, and centrifuged at 3,000 rpm to remove insoluble material. Slides were incubated at 37°C in a humidified chamber for 4 h for assessment of total PA activity and for 24 h in the presence of uPA-specific inhibitor amiloride (2 mM, Sigma-Aldrich) for assessment of tPA activity. Caseinolysis was monitored by examination under a dark field microscope.

Gelatin Zymography Assay
Choroidal neovascularization was induced in mice by multiple laser burns as described above. Animals were sacrified at day 3 and the eyes were enucleated. The posterior segments were cut out and snap frozen in liquid nitrogen. Frozen tissues were then pulverized in liquid nitrogen, homogenized in buffer (0.1 M Tris-HCl pH 8.1, 0.4% Triton X100) and centrifuged for 20 minutes at 5000 X g. The pellets were discarded. Aliquots of supernatants were mixed with SDS sample buffer and electrophoresed directly..

C- CONCLUSIONS

Plasminogen activator inhibitor type-1 (PAI-1) is the main physiological inhibitor of uPA and tPA. It not only regulates the proteolytic activity of uPA but also determines the level of uPA bound to its cell surface receptor (uPAR) by promoting the rapid endocytosis of the trimolecular uPA-uPAR-PAI-1 complex. We have reported previously that deficient PAI-1 expression in mice prevented the development of experimental CNV, which was restored when systemic and local PAI-1 expression was achieved by intravenous injection of a replication-defective adenoviral vector expressing PAI-1 cDNA. However, high doses of PAI-1 were equally efficient in inhibiting CNV development (Lambert et al, submitted) indicating that in this murine model of exsudative AMD, finely tuned fibrinolysis was a key element. We show here immunohistochemically that in the absence of uPA, tPA or Plg, excessive accumulation of fibrinogen/fibrin takes place at the level of the laser-induced trauma even in the presence of MMP-s activity. These fibrin deposits might impose a physical barrier to several components of normal CNV (endothelial cells, fibroblasts and monocytes) that cannot be resolved without plasmin-mediated fibrinolysis. Taken together, these results suggest that in the choroid, the angiogenic program is more dependent on the PA/plasminogen axis than on the reliance on MMP-driven fibrinolysis. This is in line with our recent observations in MMP-9 deficient mice showing that, while MMP-9 was expressed and active during CNV formation, its absence induced only a modest reduction in neovascularization.
Choroidal capillaries forming pathological neovascular membranes appear to be exquisitely sensitive to variations in the proteolytic balance. Both excessive fibrinolysis (such as occuring in PAI-1 deficiency) and defective one (the result of either isolated Plg/PA deficiency, or excessive PAI-1 levels) prevents the development of neovascularization and could be proposed, if appropriately controlled, as an antiangiogenic pharmacological strategy.

MODEL OF CHOROIDAL VASCULARIZATION: Green Argon Laser Impacts.

532 nm
50 µm ∅
0.05 sec
400mW

Quantification of neovascularization.

B = the thickness from the bottom of the choroid to the top of the neovascular area.
C= thickness of intact adjacent choroid.

CNV development *in vivo* in $uPA^{-/-}$, $uPAR^{-/-}$, and $Plg^{-/-}$ mice.

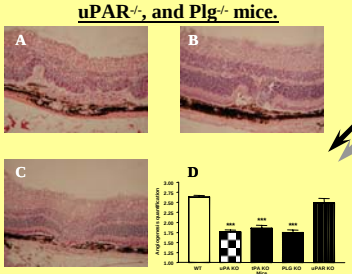

CNV at the site of laser-induced trauma was very restricted in $uPA^{-/-}$ (B), $tPA^{-/-}$ (not shown) and $Plg^{-/-}$ (C) mice, while robust CNV was observed in $uPAR^{-/-}$ (A) and WT (not shown) mice. A ~50 % reduction of the B/C ratio was consistently observed in uPA, tPA and Plg deficient mice ($p<0.001$) as compared to WT mice (D).

RT-PCR analysis of neovascular membranes

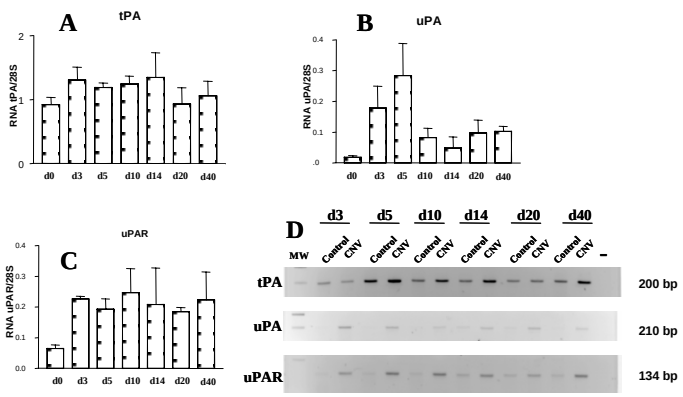

As shown on these densitometry histogram, uPA and uPAR mRNA displayed the largest the largest induction during the course of experimental murine CNV, with a decrease in expression after day 10

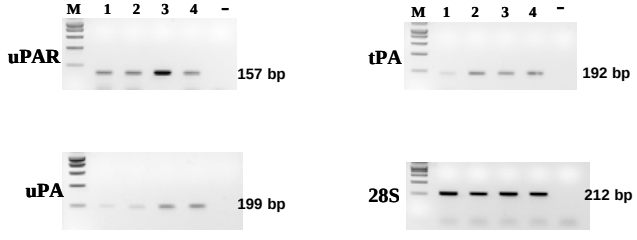

The expression of uPA, tPA and uPAR mRNA was detected in all human CNV specimens obtained during surgery.

Presence and activity of PA in murine CNV

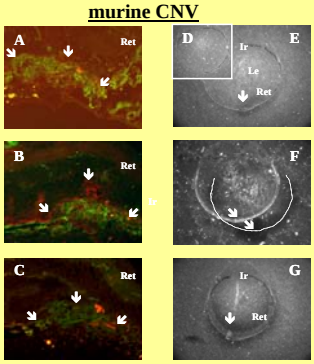

Immunohistochemical staining demonstrated the presence of uPA (A), tPA (B) and uPAR (C) proteins at the site of laser-induced injury. uPAR protein was detected both in CNV and in adjacent intact areas (B). In situ zymography in WT mice revealed that PA activity was mainly localized in and around the laser-induced CNV (E), but also present (after a longer incubation) at the level of the RPE layer (F). Caseinolytic activity was also detected when uPA was inhibited with amiloride, suggesting that tPA mediated a part of the observed proteolytic effect (G).

Fibrinogen/fibrin deposition in $uPA^{-/-}$, $tPA^{-/-}$, and $Plg^{-/-}$ mice

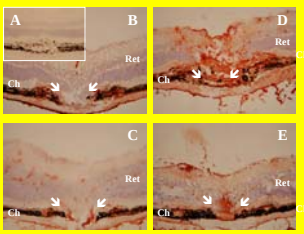

While WT (B) controls showed a modest fibrinogen/fibrin presence on the CNV growing edge, uPA (C), tPA (D) and Plg (E) deficient mice demonstrated massive accumulation of fibrinogen/fibrin both in the retinal vessels, and in the bottom of the laser-induced trauma, which had a "sealed" appearance. Negative control (A).

Gelatin zymography assay.

To investigate an influence on matrix metalloproteinase activity due to the absence of PA or Plg, the activities of MMP-2 and MMP-9 in control and deficient mice were analysed by gelatin zymography performed on the posterior segment after multiple laser-induced trauma. there was a down modulation of MMP-9 activity in Plg/PA deficient mice compared to WT controls and no evident modulation of MMP-2 compared to WT controls.